Protein-anchoring Strategy for Delivering Acetylcholinesterase to the Neuromuscular Junction

Mikako Ito[1], Yumi Suzuki[1], Takashi Okada[2], Takayasu Fukudome[3], Toshiro Yoshimura[4], Akio Masuda[1], Shin'ichi Takeda[2], Eric Krejci[5] and Kinji Ohno[1]

[1]*Division of Neurogenetics, Center for Neurological Diseases and Cancer, Nagoya University Graduate School of Medicine, Nagoya, Japan;* [2]*Department of Molecular Therapy, National Institute of Neuroscience, National Center of Neurology and Psychiatry, Tokyo, Japan;* [3]*Division of Clinical Research, Nagasaki Kawatana Medical Center, Nagasaki, Japan;* [4]*Department of Occupational Therapy, Nagasaki University School of Health Sciences, Nagasaki, Japan;* [5]*Université Paris Descartes, CNRS, UMR8194 , Paris, France*

Acetylcholinesterase (AChE) at the neuromuscular junction (NMJ) is anchored to the synaptic basal lamina *via* a triple helical collagen Q (ColQ). Congenital defects of ColQ cause endplate AChE deficiency and myasthenic syndrome. A single intravenous administration of adeno-associated virus serotype 8 (AAV8)-*COLQ* to *Colq*$^{-/-}$ mice recovered motor functions, synaptic transmission, as well as the morphology of the NMJ. ColQ-tailed AChE was specifically anchored to NMJ and its amount was restored to 89% of the wild type. We next characterized the molecular basis of this efficient recovery. We first confirmed that ColQ-tailed AChE can be specifically targeted to NMJ by an *in vitro* overlay assay in *Colq*$^{-/-}$ mice muscle sections. We then injected AAV1-*COLQ-IRES-EGFP* into the left tibialis anterior and detected AChE in noninjected limbs. Furthermore, the *in vivo* injection of recombinant ColQ-tailed AChE protein complex into the gluteus maximus muscle of *Colq*$^{-/-}$ mice led to accumulation of AChE in noninjected forelimbs. We demonstrated for the first time *in vivo* that the ColQ protein contains a tissue-targeting signal that is sufficient for anchoring itself to the NMJ. We propose that the protein-anchoring strategy is potentially applicable to a broad spectrum of diseases affecting extracellular matrix molecules.

Received 28 September 2011; accepted 31 January 2012; advance online publication 28 February 2012. doi:10.1038/mt.2012.34

INTRODUCTION

Acetylcholine (ACh) released from the nerve terminal is rapidly hydrolyzed by acetylcholinesterase (AChE) at the vertebrate neuromuscular junction (NMJ) to terminate cholinergic transmission. Three tetramers of catalytic AChE subunits are linked by a triple helical collagen Q (ColQ) to constitute a ColQ-tailed AChE.[1] The ColQ-tailed AChE is assembled in the endoplasmic reticulum and the Golgi apparatus.[2,3] ColQ carries three domains: (i) an N-terminal proline-rich attachment domain that organizes the catalytic AChE subunits into a tetramer, (ii) a collagenic domain that forms a triple helix, and (iii) a C-terminal domain enriched in charged residues and cysteines. ColQ-tailed AChE is organized in a secretory pathway, excreted, and anchored into the synaptic basal lamina using two domains of ColQ (**Figure 1**). First, the collagen domain harbors two heparan sulfate proteoglycan (HSPG)-binding domains[4] that bind to heparan sulfate proteoglycan such as perlecan in the synaptic basal lamina.[5] Second, the C-terminal domain of ColQ binds to MuSK, a muscle-specific receptor tyrosine kinase, on the postsynaptic membrane.[6] Human congenital defects of ColQ cause endplate AChE deficiency, in which the neuromuscular transmission is compromised.[7–9] Endplate AChE deficiency is an autosomal recessive disorder, which manifests as generalized muscle weakness, fatigue, amyotrophy, scoliosis, and minor facial abnormalities. Thirty-nine mutations of *COLQ* are currently registered in the Human Gene Mutation Database at http://www.hgmd.cf.ac.uk/. Ephedrine is effective for myasthenic symptoms to some extent,[10,11] though the underlying mechanisms of ephedrine efficacy remain elusive. We have developed a mouse model deficient in ColQ by deletion of the PRAD domain.[12] This strain recapitulates the phenotype of congenital myasthenic syndromes with AChE deficiency.

Gene therapy of endplate AChE deficiency is a complex issue both in humans and mice because ColQ is encoded by alternative promoters with a specific expression in subsynaptic nuclei of slow- and fast-twitch muscles.[13] The levels of AChE at the NMJ are supposed to be precisely controlled by the expression of ColQ and AChE,[14] as well as by a post-translational mechanism.[3] To treat endplate AChE deficiency in *Colq*-deficient mice, we delivered *COLQ* using adeno-associated virus (AAV) serotype 8, which has a tropism for muscles.[15] We used human *COLQ* instead of mouse *Colq* to foresee if the recombinant human *COLQ* is applicable to clinical practice in the future. Efficient rescue of AChE at the NMJ of AAV8-*COLQ*-injected mice prompted us to search for the molecular basis of these unexpected effects. We found that ColQ carries tissue-targeting signals that are necessary and sufficient to cluster AChE at the NMJ. This is the first report of a long-distance delivery of a large extracellular matrix complex over 50 nm in length and weighing over one million kDa in skeletal muscle. The findings of

Correspondence: *Kinji Ohno, Division of Neurogenetics, Center for Neurological Diseases and Cancer, Nagoya University Graduate School of Medicine, 65 Tsurumai, Showa-ku, Nagoya 466-8550, Japan, E-mail: ohnok@med.nagoya-u.ac.jp*

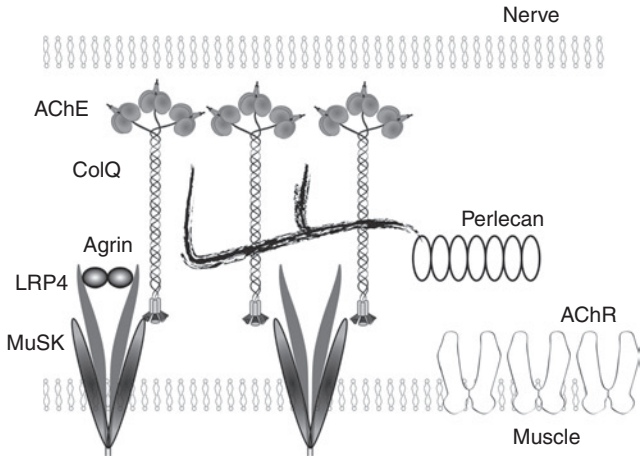

Figure 1 Schematic of anchoring of collagen Q (ColQ) to neuromuscular junction (NMJ). Twelve catalytic subunits of acetylcholinesterase (AChE) are attached to ColQ to form ColQ-tailed AChE. Two heparan sulfate proteoglycan-binding domains of ColQ are bound to perlecan. C-terminal domain of ColQ is bound to muscle-specific kinase (MuSK). Nerve-derived agrin binds to an LRP4–MuSK complex and induces rapsyn-mediated clustering of acetylcholine receptors (AChR) by phosphorylating AChR.

the present study open a new therapeutic avenue for treating many inherited defects of extracellular matrix proteins.

RESULTS

Intravenous administration of AAV8-*COLQ* normalizes motor functions of *Colq*$^{-/-}$ mice

We explored the recovery of the muscular phenotype of *Colq*$^{-/-}$ mice by viral delivery of a functional ColQ molecule. Therefore, we constructed a recombinant AAV serotype 8 carrying human *COLQ* cDNA. AAV serotype 8 (AAV8) is efficiently delivered to skeletal muscle after systemic injection.[16] We intravenously administered 1×10^{11}–2×10^{12} viral genome (vg) copies of AAV8-*COLQ* into 4-week-old *Colq*$^{-/-}$ mice. These mice exhibit muscle weakness, myasthenia, tremor, kyphosis, involuntary vocalization, and a slower growth rate than their wild-type littermates.[12] However, a single injection of 2×10^{12} vg, gradually improved their motor function to reach the level of that of wild type (**Figure 2a**). Furthermore, there were no signs of fatigue 6 weeks after the therapeutical injection (**Figure 2b**). Voluntary exercise in the treated mice also increased gradually but did not reach the level of wild type even at 5 weeks after injection (**Figure 2c**). The improved motor activities of treated mice are also demonstrated in **Supplementary Video 1**. Pairs of treated mice gave birth to *Colq*$^{-/-}$ pups and reared them to maturity. In longitudinal studies of three treated mice, all survived 18–20 months. Motor functions of the treated mice were declined at 48 weeks after injection but to the similar levels as those of wild type (**Figure 2a,c**). These observations clearly indicate the long-term therapeutic potential of a single viral injection of AAV.

AAV8-*COLQ* normalizes the neuromuscular synaptic transmission

To estimate recovery of neuromuscular transmission, we performed electrophysiological studies (**Table 1**). Treatment with

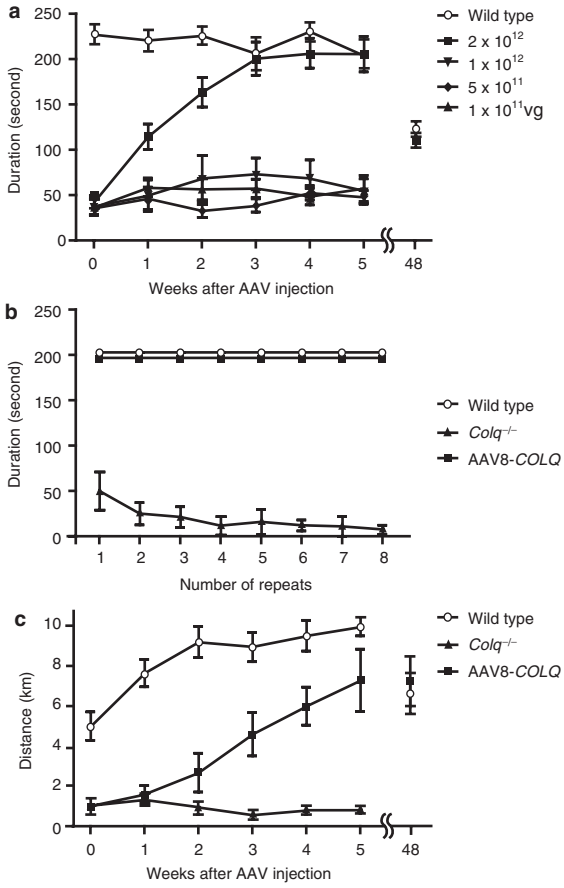

Figure 2 Exploration of motor function after intravenous injection of AAV8-*ColQ* to the tail vein of *Colq*$^{-/-}$ mice. (**a**) Motor function on the rotarod. The rotation was linearly accelerated from 0 to 40 r.p.m. in 240 seconds. Five groups of six mice were studied. Each group consisted of 4-week old mice and was either injected or not (control group) with increasing numbers of viral particles. Three weeks after their AAV8-*COLQ* injection, only the group of mice treated with 2×10^{12} vg remained on the rod as long as the wild-type littermates. Importantly, there was a progressive motor function recovery during the first 3 weeks after injection of *Colq*$^{-/-}$ mice. Symbols indicate mean and SE of six mice for each experiment. Mean and SE of the durations on the rotarod of two treated mice at 48 weeks after treatment is indicated along with that of the four age-matched wild-type mice. (**b**) Fatigue test using the rotarod was performed on three groups of a total of 18 mice. The rotation speed was fixed at 10 r.p.m. and the mice were immediately placed back on the rod each time they fell. Mice injected with 2×10^{12} vg exhibited no fatigue at 6 weeks after injection, whereas untreated *Colq*$^{-/-}$ mice fell increasingly more rapidly off the rod. (**c**) Voluntary movements were quantified by a counter-equipped running wheel. Plots show mean and SE of the number of rotations over 24 hours in each group of six mice (wild type, *Colq*$^{-/-}$, and AAV8-*COLQ*). Only the group of mice treated with 2×10^{12} vg increased the number of rotations every week but they did not reach the level of wild-type mice at 5 weeks after injection. Mean and SE of the number of rotations of two treated mice at 48 weeks after treatment is indicated along with that of the four age-matched wild-type mice. AAV8, adeno-associated virus serotype 8; ColQ, collagen Q.

AAV8-*COLQ* reduced decrements of the compound muscle action potentials in response to repetitive nerve stimulation at 2 Hz, reduced the amplitudes of miniature endplate potentials (MEPPs), shortened the miniature endplate potential decay time constants (**Figure 3**), and acquired responses to neostigmine. Endplate potential quantal content, which was decreased in

Table 1 Repetitive nerve stimulation and microelectrode studies

	Wild type	Wild type with neostigmine	*Colq*$^{-/-}$	*Colq*$^{-/-}$ with neostigmine	Treated *Colq*$^{-/-}$	Treated *Colq*$^{-/-}$ with neostigmine
Repetitive nerve stimulation[a]	0.92 ± 0.01* (2)	n.a.	0.58 ± 0.05 (3)	n.a.	0.76 ± 0.02* (3)	n.a.
EPP quantal content[b]	39.8 ± 2.3** (18)	n.a.	28.2 ± 1.8 (19)	n.a.	24.1 ± 1.6 (18)	n.a.
MEPP amplitude (mV)[c]	0.77 ± 0.04** (31)	1.52 ± 0.12 (18)	1.52 ± 0.11 (19)	1.52 ± 0.07 (10)	0.68 ± 0.02** (25)	0.98 ± 0.05** (24)
EPP amplitude (mV)[d]	30.6	n.a.	42.9	n.a.	16.4	n.a.
MEPP decay time (ms)[c]	1.77 ± 0.06** (31)	2.27 ± 0.08** (18)	3.07 ± 0.12 (19)	2.99 ± 0.09 (10)	2.45 ± 0.08** (25)	3.66 ± 0.09** (24)

Abbreviations: AChR, acetylcholine receptors; ColQ, collagen Q; EPP, endplate potential; MEPP, miniature endplate potential; n.a., not applicable.
Values represent mean ± SE. T = 29 ± 0.5 °C for EPP and MEPP recordings. Numbers in parenthesis indicate the number of recordings for repetitive nerve stimulation and the number of EPs from one or two mice for the other assays.
[a]Repetitive nerve stimulations were performed at 2 Hz, and the relative areas of compound muscle action potential (CMAP) of the fourth to the first stimulations are indicated. [b]Quantal content of EPP at 0.5 Hz stimulation corrected for resting membrane potential of –80 mV, nonlinear summation, and non-Poisson release. As the quantal contents of EPP are higher than 10, corrected values are indicated according to Cull-Candy *et al.*[45c] Normalized for resting membrane potential of –80 mV and a mean muscle fiber diameter of 55 µm. The actual fiber diameters were 45 ± 3.6 µm (mean ± SD, $n = 31$) for wild-type mice, 43 ± 3.0 µm ($n = 19$) for *Colq*$^{-/-}$ mice, and 46 ± 4.2 µm ($n = 25$) for the treated *Colq*$^{-/-}$ mice. [d]Estimated EPP amplitude is the product of the EPP quantal content and the MEPP amplitude. As AChR was partly blocked with curare for EPP recordings and not for MEPP recordings, we could not directly measure EPP amplitudes. Predicted low EPP amplitudes in treated mice suggest that the improvement of motor function was likely due to amelioration of depolarization block and/or of endplate myopathy.
*$P < 0.05$ and **$P < 0.001$ compared to *Colq*$^{-/-}$ mice by Student's *t*-test.

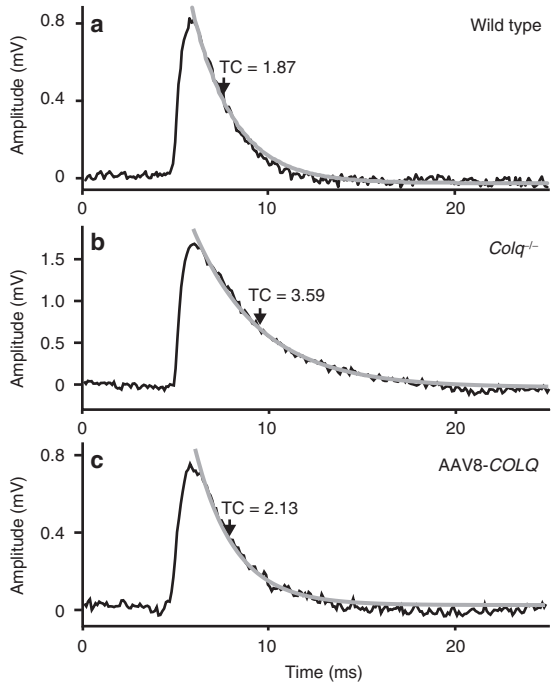

Figure 3 Representative miniature endplate potential (MEPP) recordings of diaphragm muscles of (a) wild type, (b) *Colq*$^{-/-}$, and (c) AAV8-*COLQ*-treated mice. (**b**) *Colq*$^{-/-}$ mice have higher MEPP amplitude and a longer decay time constant (TC) than (**a**) wild-type mice. AAV8-*COLQ* treatment shortened the decay TC and lowered the MEPP amplitude. Gray lines represent fitted exponential decay curves. AAV8, adeno-associated virus serotype 8; ColQ, collagen Q.

Colq$^{-/-}$ mice, was further decreased by the treatment, in contrast to our expectation.

Human ColQ-tailed AChE is anchored to the mouse NMJ *in vivo*

To further evaluate that the rescue was due to restitution of AChE at the NMJ, we used histological methods to visualize ColQ and AChE on muscle sections (**Figure 4a–c**). ColQ and AChE were colocalized to acetylcholine receptors (AChR) at the NMJ, confirming that ColQ-tailed AChE was specifically clustered to the target tissue. Although, we failed to observe improvement of motor functions with 1×10^{12} vg or less (**Figure 2a**), we still detected ColQ and AChE at NMJs with smaller amounts (data not shown). This suggests that a certain amount of viral genomes is required to exhibit improvement of motor deficits.

The ultrastructural morphology of treated mice also improved compared with age-matched *Colq*$^{-/-}$ mice (**Figure 4d–f**). The NMJ ultrastructures were variable from one to another in wild type, *Colq*$^{-/-}$, and treated mice, and we quantified the electron micrograph pictures (**Supplementary Table S1**). Quantitative analysis of presynaptic ultrastructures demonstrated that, in soleus slow-twitch muscle, Schwann cell invagination was mitigated, which increased the nerve terminal length, but the nerve terminal area remained essentially the same. Postsynaptic area and postsynaptic membrane length were also increased in soleus muscle of treated mice. In the extensor digitorum longus fast-twitch muscle, however, significant improvement was observed only in the ratio of enwrapped nerve terminal. Thus, the morphological improvements were more prominent in the soleus rather than in extensor digitorum longus muscles.

AAV8-*COLQ* restores the amount of ColQ-tailed AChE in the muscle to 89.3% of wild type

To estimate the efficiency of intravenous administration of AAV8-*COLQ*, we quantified the amount of the transduced *COLQ* mRNA, as well as ColQ-tailed AChE, in the muscle. We estimated the amount of *COLQ* mRNA in hindlimbs by a TaqMan probe, and found that the treated mice expressed the transduced *COLQ* at 92.5 ± 47.8% (mean ± SE, $n = 4$) of wild type. ColQ-tailed AChE from hindlimbs of the treated mice was fractionated by sucrose density-gradient ultracentrifugation. Sedimentation analysis revealed that AAV8-*COLQ* muscles have similar peaks of ColQ-tailed AChE species as those of wild type (**Figure 5a–c**). We also quantified the amount of globular AChE and ColQ-tailed AChE in gastrocnemius muscles of treated mice (**Figure 5d**). As previously reported, the amount of globular AChE was slightly lower in *Colq*$^{-/-}$ mice,[12] and this was normalized by treatment

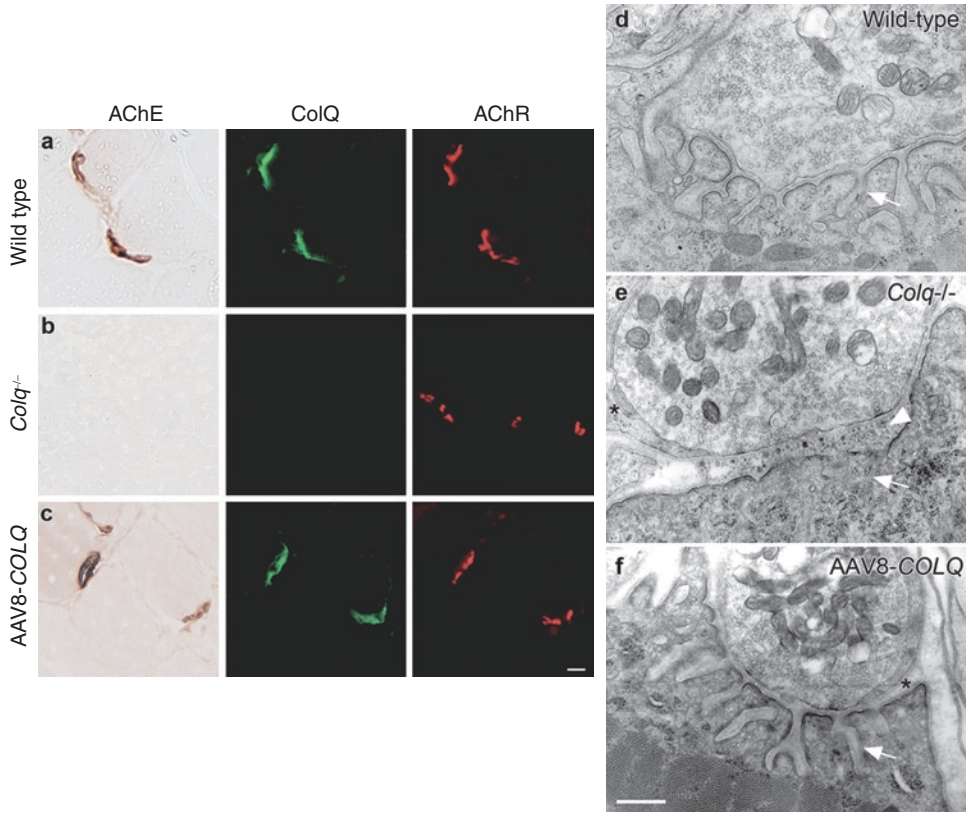

Figure 4 Histologies and ultrastructures of the neuromuscular junctions (NMJs). Localization of acetylcholinesterase (AChE) activity, collagen Q (ColQ), and acetylcholine receptors (AChR) in quadriceps muscles of (a) wild type, (b) *Colq*$^{-/-}$, and (c) AAV8-*COLQ* mice. Mice treated with 2 × 10^{12} vg of intravenous AAV8-*COLQ* express ColQ-tailed AChE at NMJ. AChE is stained for its activity. ColQ and AChR are detected by the polyclonal anti-ColQ antibody and α-bungarotoxin, respectively. Bar = 10 µm (**a–c**). Representative stainings of six mice in each group are indicated. Ultrastructures of soleus muscle NMJ (**d–f**). (**e**) *Colq*$^{-/-}$ mice show simplified synaptic clefts (arrow) and widening of the synaptic space (arrow head), whereas the NMJ ultrastructure of AAV8-*COLQ* mice (**f**) is indistinguishable from that of wild type (**d**). AAV8-*COLQ* mice still have small nerve terminals and invaginated Schwann cells (*). Bar = 1 µm (**d–f**). Representative ultrastructures of 27–41 electron micrograph (EM) pictures (see **Supplementary Table S1**) are indicated. AAV8, adeno-associated virus serotype 8.

with AAV8-*COLQ*. Treatment with AAV8-*COLQ* also restored ColQ-tailed AChE to 89.3 ± 9.6% (mean ± SD, $n = 4$) of wild type at 6 weeks after treatment. We also quantified ColQ-tailed AChE at 48 weeks after treatment and found that the amount was still 81.8 ± 21.6% (mean ± SD, $n = 2$) of the age-matched wild-type mice ($n = 3$). Although soleus slow-twitch muscle exhibited prominent improvement with the ultrastructural analysis, the available amount of soleus muscle was too small for the biochemical assay.

We also examined whether ColQ-tailed AChE was produced in the liver because AAV8 efficiently transduces hepatocytes.[15] AAV8-*COLQ* increased the *COLQ* mRNA level in the liver from 3.4 ± 0.34% (mean ± SE of five wild-type mice) to 61.3 ± 12.6% (mean ± SE of five treated mice) compared to those in the muscle of wild-type mice ($n = 5$). The *Ache* mRNA levels in the liver of wild type, *Colq*$^{-/-}$, and treated mice, however, were estimated to be <0.5% of that in wild-type muscle. The *Ache* mRNA levels in the liver were too low to be accurately quantified by real-time reverse transcription-PCR. Sedimentation profiles revealed no peaks of ColQ-tailed AChE in the liver of either wild type, *Colq*$^{-/-}$, or treated mice (**Supplementary Figure S1a–c**). This was probably due to lack of *Ache* expression. Globular AChE species observed in the sedimentation analysis was likely to represent AChE on the erythrocyte cell membrane.[17] These data suggest that AAV8-*COLQ* did not induce expression of ColQ-tailed AChE in the liver.

Local intramuscular injection of AAV8-*COLQ* expresses ColQ-tailed AChE at NMJs of noninjected limbs

Prominent improvements that we observed in AAV8-*COLQ*-treated mice raised a possibility that ColQ-tailed AChE moved from the transduced muscle cells to other muscle cells. We thus tested this possibility in the following experiments.

First, we have previously reported that the human recombinant ColQ-tailed AChE can be anchored to the synaptic basal lamina of the frog NMJ.[18] We tested this anchoring using mouse NMJs. We purified ColQ-tailed AChE expressed in HEK293 cells and incubated this with a section of skeletal muscle from *Colq*$^{-/-}$ mice. As expected, ColQ and AChE were detected at the mouse NMJ (**Supplementary Figure S2**), which supports the notion that ColQ-tailed AChE can be moved and anchored to the target *in vitro*.

Next, we tested whether ColQ-tailed AChE moved from the transduced muscles to the nontransduced muscles. We injected AAV8-*COLQ* to the left anterior tibial muscle. As expected, AChE and ColQ were rescued at the NMJs of the injected muscle. In addition, AChE and ColQ were also detected at all the examined

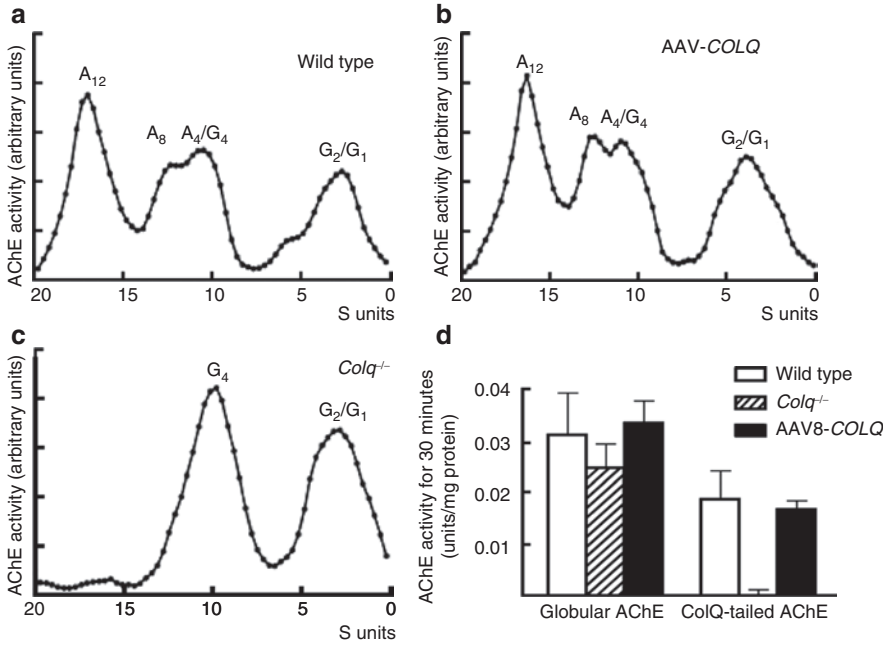

Figure 5 Quantification and biochemical analysis of acetylcholinesterase (AChE) recovery in muscles. Intravenous injection of 2×10^{12} vg of AAV8-*COLQ* into (**b**) *Colq*$^{-/-}$ mice gives rise to a sedimentation profile that is identical to that of (**a**) wild type, whereas (**c**) *Colq*$^{-/-}$ mice carry no collagen Q (ColQ)-tailed AChE. A_4, A_8, and A_{12} species carry 4, 8, and 12 AChE catalytic subunits attached to a triple helical ColQ. G_1, G_2, and G_4 species carry 1, 2, and 4 AChE catalytic subunits but without ColQ. A representative profile of three experiments is indicated. (**d**) Quantification of globular and ColQ-tailed AChE species (mean and SD, $n = 4$). The activity of ColQ-tailed AChE in the skeletal muscle of AAV8-*COLQ* mice is restored to 89 ± 10% of that of wild type. AAV8, adeno-associated virus serotype 8.

NMJs in noninjected muscles (data not shown). These results, however, could not exclude the possibility that AAV8-*COLQ* had been delivered to noninjected muscles in the form of a virus.

Local intramuscular injection of AAV1-*COLQ-IRES-EGFP* expresses ColQ-tailed AChE at NMJs of noninjected limbs

To reduce systemic delivery of AAV8 and to identify infected cells, we packed *COLQ* cDNA into the AAV serotype 1 (AAV1) that is known to transduce the injected muscle fibers locally.[19] In addition, we fused *COLQ* and internal ribosome entry site (*IRES*)-*EGFP* to express green fluorescent protein (GFP) in transduced cells synthesizing ColQ. We injected 2×10^{11} vg of AAV1-*COLQ-IRES-EGFP* into the left anterior tibial muscle of *Colq*$^{-/-}$ mice, while blocking the blood flow with a tourniquet for 20 minutes to restrict the distribution of the virus. The transduction efficiencies of AAV1-*COLQ-IRES-EGFP* were as follows: left anterior tibial muscle, 1.70 ± 0.29 viral copies per nucleus; right gastrocnemius muscle, 0.00100 ± 0.00079 copies; and bilateral brachial muscles, 0.00126 ± 0.00058 copies (mean ± SD, $n = 3$). Although only a fraction of the injected AAV1-*COLQ-IRES-EGFP* moved to noninjected limbs, we observed colocalization of ColQ and AChE at all the examined NMJs of right gastrocnemius, right tibialis anterior, both triceps, and both biceps in four examined mice (**Figure 6a**). We analyzed a total of 200–400 NMJs per muscle. In contrast, expression of intracellular enhanced GFP (EGFP) was not observed in noninjected limb muscles. We also quantified ColQ-tailed AChE in the noninjected bilateral forelimbs and right hindlimb, and found that the amounts were 21.5 ± 10.2% and 28.4 ± 10.0% (mean ± SD, $n = 4$), respectively, of those of wild type (**Figure 6b**).

ColQ-tailed AChE protein reaches and binds to remote NMJs

The presence of ColQ in noninjected muscles strongly suggests that the ColQ-tailed AChE is assembled intracellularly in one muscle and has moved to noninjected muscles, where it is anchored to the NMJs. To directly test this possibility, the gluteus maximus muscles of 5-week-old *Colq*$^{-/-}$ mice ($n = 4$) were injected daily with 2 µg of recombinant human ColQ-tailed AChE for 7 days. Histological analysis revealed the presence of ColQ and AChE in all of the examined NMJs from triceps muscles (**Figure 7a**). Quantitative analysis of ColQ signal intensities at the NMJs of noninjected triceps demonstrated that the ColQ-positive areas normalized for the AChR-positive area per NMJ became indistinguishable from that of wild type (**Figure 7b**). Furthermore, the ColQ signal intensity normalized for the AChR area per NMJs reached ~41.6% of that of wild type (**Figure 7c**). The *Colq*$^{-/-}$ mice could not hang on the wire at all, but the protein-injected mice acquired the ability to hang on the wire for two or more minutes from the fourth day of injection.

DISCUSSION

Effective and persistent gene therapy of ColQ with a single intravenous injection of AAV8-*COLQ*

We present an efficient and persistent recovery of AChE at the NMJ after a single intravenous administration of AAV8-*COLQ* in a *Colq*$^{-/-}$ mouse model of congenital myasthenic syndrome

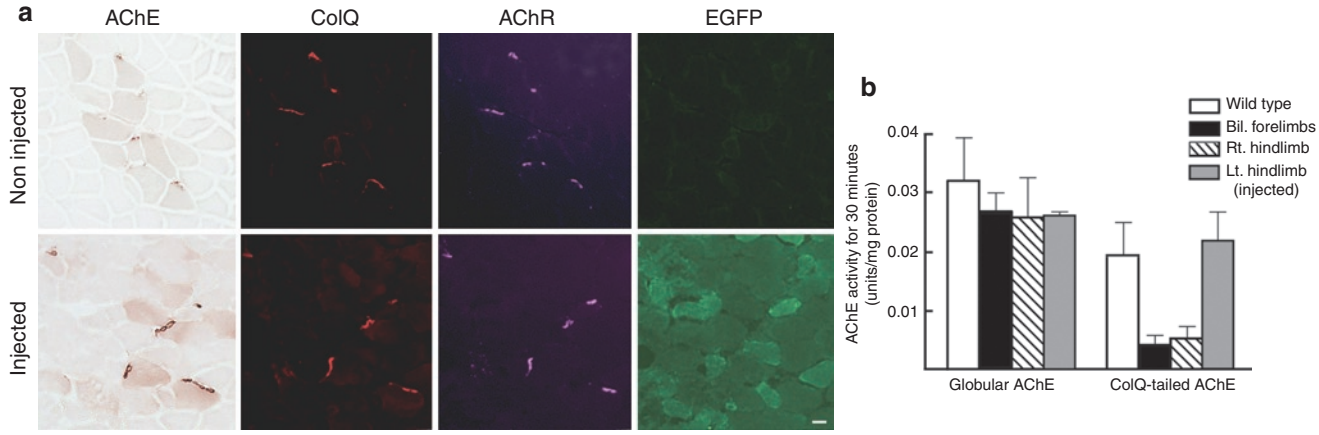

Figure 6 Intramuscular injection of 2 × 10^{11} vg of AAV1-*COLQ-IRES-EGFP* into the left anterior tibial muscle of *Colq*$^{-/-}$ mice. (**a**) Acetylcholinesterase (AChE) activity and collagen Q (ColQ) are colocalized to the acetylcholine receptors (AChR) in the injected muscle, as well as in the noninjected triceps muscle, although the signal intensities are not as high as those of the injected muscle. In contrast to ColQ, an intracellular molecule, enhanced green fluorescent protein (EGFP), is expressed only in the injected muscle, but not in the noninjected muscle. Bar = 10 µm. (**b**) Quantification of globular and ColQ-tailed AChE species of skeletal muscles (mean and SD, n = 4). In the injected left hindlimb, the activity of ColQ-tailed AChE is similar to that of wild type. In the noninjected both forelimbs and right hindlimb, the activities are 21.5 and 28.4% of wild type, respectively. AAV1, adeno-associated virus serotype 1.

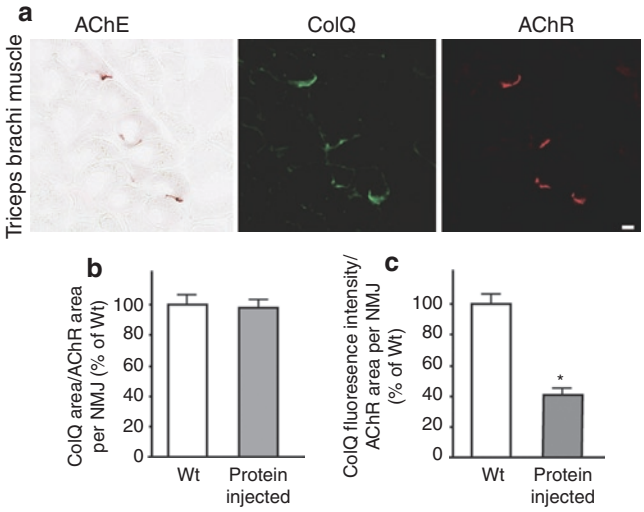

Figure 7 Injection of purified recombinant human collagen Q (ColQ)-tailed acetylcholinesterase (AChE). (**a**) Daily injection of 0.2 µg human recombinant ColQ-tailed AChE into the gluteus maximus muscles of *Colq*$^{-/-}$ mice rescues AChE activity and ColQ in the noninjected triceps where they are colocalized to acetylcholine receptors (AChR). Bar = 10 µm. (**b**) The size of ColQ-positive area is normalized for the size of AChR-positive area at the neuromuscular junctions (NMJs) of noninjected triceps. (**c**) Signal intensities of ColQ at the NMJs of noninjected triceps. Mean and SE are indicated. WT, wild-type mice, number of NMJs = 43; Protein injected, mice injected with ColQ-tailed AChE, number of NMJs = 42. *P < 0.001. Signal intensities are normalized to that of *Colq*$^{-/-}$ mice. Quantitative analyses were performed with the BZ-9000 microscope and the Dynamic Cell Count software BZ-H1C (Keyence).

with deficit in AChE. We observed ColQ-tailed AChE at all of the NMJs examined and the amount of the anchored AChE reached 89.3% of the wild-type level. The improved motor functions lasted at least 48 weeks after treatment and the treated mice survived 18–20 months, which is in contrast to at most 6-month lifespan of *Colq*$^{-/-}$ mice.[12] Although >99.5% of the vector genome stays episomal in mouse muscles even at 57 weeks after injection,[20,21] expression of the transgene in skeletal muscle lasts for 1.0–1.5 years without a decline in immunocompetent mice.[22,23] Our studies also underscore the long-lasting expression of the transgene delivered by AAV.

Rat *Colq*[24] and human *COLQ*[7] have two distinct promoters and generate ColQ1 and ColQ1a transcripts, which respectively include exon 1 and exon 1a and encode distinct signal peptides. A nerve-derived factor, calcitonin gene-related peptide, controls the expression of ColQ1a at the NMJs of fast-twitch muscles. However, in slow-twitch muscles, expression of ColQ1 occurs throughout the muscle fibers and is controlled by Ca^{2+}/calmodulin-dependent protein kinase II and myocyte enhancer factor 2.[24,25] As our viral construct was driven by the cytomegalovirus promoter, spatial and temporal regulation of ColQ expression should have been lost. In addition, our construct expressed ColQ1 and not ColQ1a, which was expected to be physiological for slow-twitch muscle but not for fast-twitch muscles. The prominent ultrastructural improvement in slow-twitch muscles rather than fast-twitch muscles may be partly because AAV8-*COLQ* encodes ColQ1 and not ColQ1a. This also suggests that the N-termini of ColQ1 and 1a have different functions. The pattern of ColQ expression resulting from our strategy was not physiological in three ways: (i) lack of subsynaptic nuclei-specific expression of ColQ, (ii) a ubiquitous cytomegalovirus promoter, and (iii) the exclusive expression of ColQ1. Despite these features, the motor and the synaptic functions are improved; AChE is locally accumulated at the NMJ in our treated mice. This suggests that the precise genetic control of the expression of ColQ is not the key factor for clustering of AChE and tissue-targeting signals of ColQ are sufficient to functionally restore AChE at the NMJ.

The protein-anchoring therapy

Although ColQ-tailed AChE in the serum of either wild type, *Colq*$^{-/-}$, or treated mice was less than a detection threshold in the

sedimentation analysis (**Supplementary Figure S1d–f**), anchoring of ColQ-tailed AChE to remote NMJs was supported by two lines of evidence: local intramuscular injections of AAV1-*COLQ-IRES-EGFP* (**Figure 6**) and of the purified recombinant ColQ-tailed AChE protein complex (**Figure 7**). In either case, AChE at the NMJ of the noninjected muscle originates from ColQ-tailed AChE arising from another source; not from local secretion and retention of ColQ-tailed AChE synthesized by subsynaptic nuclei followed by assembly and maturation in the postsynaptic area as in wild-type mice. The overlay of recombinant ColQ-tailed AChE *in vitro* either on normal muscle tissue sections of frog[5,18] or of *Colq*$^{-/-}$ mouse (**Supplementary Figure S2**) demonstrates that ColQ harbors a signal that targets AChE to the NMJ. The dual interactions of ColQ with MuSK[6] and perlecan,[5] which are both required in the overlay experiment,[18] are likely to restrict ColQ to the NMJ. In endplate AChE deficiency, point mutations that affect the binding of ColQ to MuSK prevent the accumulation of AChE.[18] Although no mutation has been reported at the heparan sulfate proteoglycan-binding domains of ColQ in endplate AChE deficiency, the reduction of perlecan mimicking Schwartz–Jampel syndrome reduces the level of AChE and ColQ at the NMJ.[26,27] All of these observations suggest that the combination of MuSK and perlecan determines the number of ColQ-tailed AChE anchored at the NMJ. This notion was previously termed as "molecular parking lots" by Rotundo and colleagues.[28]

ColQ-tailed AChE is a nanostructure made of a rigid collagen of 50-nm length and three AChE tetramers. ColQ-tailed AChE is apparently able to move from one muscle to another as demonstrated by clustering in the triceps muscle after protein injection into the gluteus. A similar approach is inherently employed by nature, as exemplified by fibronectin that is ubiquitously present in extracellular matrices and is largely derived from liver.[29] Injection of a protein complex is reported with laminin-111.[30] An intramuscularly or intraperitoneally injected laminin-111 is distributed to the basal lamina of skeletal and cardiac muscles in an mdx-mouse model of Duchenne muscular dystrophy. In contrast to our strategy, laminin-111 is not expressed or accumulated in normal or dystrophic adult muscles. Their studies exploit an ectopic deposition of laminin-111 to induce expression of α_7-integrin that stabilizes the sarcolemma of dystrophic muscle fibers.

The ColQ must be synthesized in cells that produce a splice variant T of AChE for obtaining the correct assembly of the complex.[2] A single muscle fiber harbors hundreds of nuclei that are functionally compartmentalized, and a molecule expressed in a single nucleus goes through the muscle fiber only for a short distance.[31,32] Thus, the multinucleation of muscle fibers is unlikely to have contributed to the restoration of function in the *Colq*$^{-/-}$ mice of our study. Similar specific clustering of a muscle-generated protein to the NMJ has been reported with laminin β2.[33] When laminin β2 is expressed throughout muscle fibers by the MCK promoter in transgenic mice, it is clustered at the NMJ.

The inability to achieve efficient and specific delivery of a transgene to the target tissue often prevents the application of gene therapy to model animals and patients.[34] Here, we propose the protein-anchoring strategy that provides a new therapeutic approach for congenital defects of extracellular matrix proteins.[35] The potential candidate molecules of the protein-anchoring therapy include laminin α2 causing laminin-α2-deficient congenital muscular dystrophy,[36] perlecan causing Schwartz–Jampel syndrome,[26,37] and collagen VI causing Ullrich syndrome.[38] It should be emphasized that this strategy can be potentially used for a huge number of diseases caused by mutations of genes encoding proteins of the extracellular matrices in general.

MATERIALS AND METHODS

Preparation of AAV carrying COLQ. Human *COLQ* cDNA[7] was cloned into pAAV-MCS (AAV Helper-Free system; Stratagene, Santa Clara, CA) that carries the cytomegalovirus promoter to obtain a pAAV-*COLQ*. We also inserted *IRES-EGFP* to make pAAV-*COLQ-IRES-EGFP*. To make AAV8-*COLQ*, HEK293 cells were cotransfected with the following plasmids: the proviral vector plasmid pAAV-*COLQ*, the AAV8 chimeric helper plasmid pRC8, and the adenoviral helper plasmid pHelper (Stratagene) using calcium phosphate coprecipitation method.[39] To make AAV1-*COLQ-IRES-EGFP*, we transfected HEK293 cells with pAAV-*COLQ-IRES-EGFP,* the AAV1 chimeric helper plasmid pRep2Cap1, and pHelper. The AAV particles were concentrated by CsCl gradient ultracentrifugation for 3 hours[40] and further purified with the quick dual ion-exchange procedures.[41] The viral titer was estimated by quantitative PCR in real-time using MX3000p (Stratagene).[42]

Administration of AAV carrying COLQ to Colq$^{-/-}$ mice. All animal studies were approved by the Animal Care and Use Committee of the Nagoya University Graduate School of Medicine. For intravenous administration, 1×10^{11}–2×10^{12} vg of AAV8-*COLQ* were injected into the tail vein of 4-week-old *Colq*$^{-/-}$ mice.[12] For intramuscular administration, 2×10^{11} vg of AAV1-*COLQ-IRES-EGFP* were injected into the left anterior tibial muscle of 4-week-old *Colq*$^{-/-}$ mice. The left proximal thigh was tightly ligated with a tourniquet for 20 minutes during intramuscular injection to prevent vascular delivery of viral particles throughout the body.

Motor activity tests. Muscle weakness and fatigability were measured with a rotarod apparatus (Ugo, Basile, Italy). Mice were first trained three times to be accommodated to the task. Mice were consecutively examined three times and were allowed to take a rest for 1 hour between individual tasks.

Running-wheel activity was used to quantify voluntary exercises. Each mouse was placed in a standard cage equipped with a counter-equipped running wheel (diameter, 14.7 cm, width, 5.2 cm; Ohara Medical, Tokyo, Japan). The running distances were recorded using the counter every 24 hours.

Histology. We raised a polyclonal ColQ antibody by injecting a synthetic peptide of SAALPSLDQKKRGGHKAC, corresponding to codons 34–51 in human ColQ, into rabbits. We confirmed that the raised antibody recognized ColQ by western blotting (**Supplementary Figure S3**) and that no signal was present in a section of *Colq*$^{-/-}$ mice (**Figure 4b** and **Supplementary Figure S2**). Mice were sacrificed at 6 weeks after treatment. Skeletal muscles of mice were frozen in the liquid nitrogen-cooled isopentane and sectioned at 8-μm thick with a Leica CW3050-4 cryostat at −20 °C. Muscle sections were blocked with 5% horse serum in phosphate-buffered saline for 20 minutes and incubated with the primary antibody (1:100) for 2 hours. Sections were then incubated with a secondary antibody (1:100) for 1 hour, along with Alexa-594-conjugated α-bungarotoxin (2.5 μg/ml) (Sigma, St Louis, MO) for visualizing AChR. Anti-rabbit and anti-mouse secondary antibodies were both FITC-labeled (Vector Lab, Burlingame, CA). For AAV1-*COLQ-IRES-EGFP*, we detected ColQ using anti-rabbit secondary antibody labeled with rhodamine (1:40; Santa Cruz, Santa Cruz, CA) and localized AChR by Alexa-647-conjugated α-bungarotoxin (2.5 μg/ml; Sigma). Signals of ColQ, AChE, AChR, and EGFP were examined with BX60 (Olympus, Tokyo, Japan) or BZ-9000 (Keyence, Osaka, Japan).

Mouse AChE activity was detected by the histochemical method at 6 weeks after treatment. Muscle sections were incubated for 20 minutes at 37 °C in the reaction mixture containing 1.73 mmol/l acetylthiocholine iodide, 38 mmol/l sodium acetate, 51 mmol/l acetic acid, 6 mmol/l sodium

citrate, 4.7 mmol/l copper sulfate, 0.5 mmol/l potassium ferricyanide, and 5×10^{-5} mol/l ethopropazine (Sigma), which is an inhibitor of butyrylcholinesterase.

Sedimentation biochemical analyses. Mice were sacrificed at 6 weeks after treatment. Sedimentation analysis was performed as previously described.[7] Proteins were extracted from the muscle and liver in a detergent buffer [10 mmol/l HEPES (pH 7.2), 1% CHAPS, 10 mmol/l EDTA, 2 mmol/l benzamidine, leupeptin (20 µg/ml) and pepstatin (10 µg/ml)] containing 0.8 mol/l NaCl. The eluate was applied on a 5–20% sucrose density gradient, which was made in the detergent buffer containing 0.8 mol/l NaCl, along with β-galactosidase (16S) and alkaline phosphatase (6.1S) as internal sedimentation standards. Centrifugation was performed in a Beckman SW41Ti rotor at 4 °C for 21 hours at 38,000 r.p.m. AChE activity was assayed by the colorimetric method of Ellman in the presence of 5×10^{-5} mol/l ethopropazine.

For biochemical analysis, skeletal muscle was shattered by the Cool Mill (Toyobo, Osaka, Japan) in liquid nitrogen. We extracted globular forms of AChE into the NaCl-free detergent buffer, and ColQ-tailed AChE into detergent buffer containing 0.8 mol/l NaCl as previously described.[12] AChE activity was assayed using AChE-Specific Assay kit (Dojindo, Kumamoto, Japan) or the Ellman method and normalized by Torpedo AChE activity (Sigma).

Microelectrode studies. Phrenic nerve-diaphragm preparations were obtained from three wild type, three *Colq*$^{-/-}$, and three AAV8-*COLQ*-treated mice at 8 weeks of age, which corresponds to 4 weeks after treatment. We stimulated the sciatic nerve at 2 Hz and recorded compound muscle action potentials of gastrocnemius muscles using a needle electrode under deep anesthesia. For technical reasons, we could not analyze the limb muscles that we used in the other assays. After mice were sacrificed, miniature endplate potentials and evoked EPPs were recorded as described elsewhere.[43] Neostigmine methylsufate (Elkins-Sinn, Cherry Hill, NJ) was used at a concentration of 10^{-6} g/ml in the bath to block cholinesterases. We employed the AxoGraph × 1.1.6 (AxoGraph Scientific, Sydney, Australia) for data analysis.

Electron microscopy. For electron microscopy, extensor digitorum longus and soleus muscles were fixed in ice-cold 3% glutaraldehyde buffered with 0.1 mol/l cacodylate buffer (pH 7.3) at 4 weeks after treatment. The endplate-rich region of the muscle was refixed in 2% OsO_4 in cacodylate buffer, dehydrated, and embedded in Epon812.

All thin sections were cut transversely, stained with lead citrate, and photographed in a JEM 1,200 EX electron microscopy. Morphometric analysis of the motor endplate was performed following the procedure of Engel and Santa,[44] and included the following: (i) presynaptic membrane length, in µm; (ii) nerve terminal area, in µm^2; (iii) number of synaptic vesicles per unit area, in numbers per µm^2; (iv) length of processes of Schwann cells on presynaptic membrane, in µm; (v) percentage of totally enwrapped nerve terminal by processes of Schwann cells; (vi) postsynaptic area of folds and clefts associated with a given nerve terminal, in µm^2; (vii) postsynaptic membrane length associated with a given nerve terminal, in µm; (viii) postsynaptic membrane length per unit postsynaptic area (postsynaptic membrane density), derived by dividing the value of (vii) by that of (vi), in µm per µm^2; (ix) postsynaptic to presynaptic membrane ratio. Endplates were localized and analyzed by established methods, and peroxidase-labeled α-bungarotoxin was used for the ultrastructural localization of AChR.[45] The images were quantified using the NIH Image 1.62 software (National Institutes of Health).

Expression and purification of recombinant ColQ. The plasmids that previously introduced human *COLQ* and human *ACHE* cDNAs into a pTargeT (Promega, Madison, WI)[7] were cotransfected into HEK293 cells. Proteins were extracted from the cells in Tris–HCl buffer [50 mmol/l Tris–HCl (pH 7.0), 0.5% Triton X-100, 0.2 mmol/l EDTA, leupeptin (2 µg/ml), and pepstatin (1 µg/ml)] containing 1 mol/l NaCl. The extracts were loaded onto HiTrap Heparin HP columns (GE Healthcare, Buckinghamshire, UK). The concentration of purified recombinant ColQ-tailed AChE was equivalent to ~4 µg/ml Torpedo AChE. We injected 50 µl of the purified ColQ-tailed AChE in phosphate-buffered saline daily into the gluteus maximus muscles of 5-week-old *Colq*$^{-/-}$ mice for a week. Mice were given a single intraperitoneal injection of 300 mg/kg cyclophosphamide monohydrate (10 mg/ml in saline) at 24 hours after the first ColQ-tailed AChE injection to suppress immunoreaction against the recombinant human protein.[46] After 7 days, mice were sacrificed and brachial muscles were stained for ColQ molecule and AChE activity as described above.

Real-time PCR/reverse transcription-PCR. For expression analysis, total RNAs from skeletal muscle and liver cells were extracted using the RNeasy Mini kit (Qiagen, Hilden, Germany) with *DNase*I and proteinase K treatment according to the manufacturer's instructions. First-stranded cDNA was synthesized using the ReverTra Ace reverse transcriptase (Toyobo). Expressions of human *COLQ*, mouse *Colq*, and mouse *Ache* were analyzed using the TaqMan (Applied Biosystems, Foster city, CA) probes and primers in LightCycler 480 (Roche, Mannheim, Germany). We also quantified 18S rRNA for normalization.

To quantify the transduction efficiency, total DNA was extracted from skeletal muscle and liver using the QIAamp DNA Mini Kit (Qiagen). The amount of viral genome was quantified by real-time PCR using a TaqMan probe targeting to human *COLQ*, as well as to mouse *Tert* encoding telomerase reverse transcriptase to normalize for the cell numbers.

SUPPLEMENTARY MATERIAL

Figure S1. Sedimentation analyses of AChE in the liver and serum.
Figure S2. Binding of human ColQ-tailed AChE proteins to the NMJ in muscle section of *Colq*$^{-/-}$ mice.
Figure S3. Western blot of a newly raised rabbit polyclonal anti-ColQ antibody (1:1,000).
Table S1. Morphometric analysis of endplate ultrastructures.
Video 1. First part: Two *Colq*$^{-/-}$ mice treated with an intravenous administration of 2×10^{12} vg of AAV8-*COLQ* (right cage) move around actively.

ACKNOWLEDGMENTS

We thank James M. Wilson for providing the chimeric helper plasmid pRC8 (identical to p5E18-VD2/8) and pRep2Cap1 (identical to p5E18RXCl). This work was supported by Grants-in-Aid from the Ministry of Education, Culture, Sports, Science, and Technology of Japan, and the Ministry of Health, Labor, and Welfare of Japan, as well as by Grant from ANR maladies rares. The authors declared no conflict of interest.

REFERENCES

1. Krejci, E, Thomine, S, Boschetti, N, Legay, C, Sketelj, J and Massoulié, J (1997). The mammalian gene of acetylcholinesterase-associated collagen. *J Biol Chem* **272**: 22840–22847.
2. Rotundo, RL (1984). Asymmetric acetylcholinesterase is assembled in the Golgi apparatus. *Proc Natl Acad Sci USA* **81**: 479–483.
3. Ruiz, CA and Rotundo, RL (2009). Limiting role of protein disulfide isomerase in the expression of collagen-tailed acetylcholinesterase forms in muscle. *J Biol Chem* **284**: 31753–31763.
4. Deprez, P, Inestrosa, NC and Krejci, E (2003). Two different heparin-binding domains in the triple-helical domain of ColQ, the collagen tail subunit of synaptic acetylcholinesterase. *J Biol Chem* **278**: 23233–23242.
5. Peng, HB, Xie, H, Rossi, SG and Rotundo, RL (1999). Acetylcholinesterase clustering at the neuromuscular junction involves perlecan and dystroglycan. *J Cell Biol* **145**: 911–921.
6. Cartaud, A, Strochlic, L, Guerra, M, Blanchard, B, Lambergeon, M, Krejci, E *et al.* (2004). MuSK is required for anchoring acetylcholinesterase at the neuromuscular junction. *J Cell Biol* **165**: 505–515.
7. Ohno, K, Brengman, J, Tsujino, A and Engel, AG (1998). Human endplate acetylcholinesterase deficiency caused by mutations in the collagen-like tail subunit (ColQ) of the asymmetric enzyme. *Proc Natl Acad Sci USA* **95**: 9654–9659.
8. Donger, C, Krejci, E, Serradell, AP, Eymard, B, Bon, S, Nicole, S *et al.* (1998). Mutation in the human acetylcholinesterase-associated collagen gene, COLQ, is responsible

for congenital myasthenic syndrome with end-plate acetylcholinesterase deficiency (Type Ic). *Am J Hum Genet* **63**: 967–975.
9. Ohno, K, Engel, AG, Brengman, JM, Shen, XM, Heidenreich, F, Vincent, A *et al.* (2000). The spectrum of mutations causing end-plate acetylcholinesterase deficiency. *Ann Neurol* **47**: 162–170.
10. Bestue-Cardiel, M, Sáenz de Cabezón-Alvarez, A, Capablo-Liesa, JL, López-Pisón, J, Peña-Segura, JL, Martin-Martinez, J *et al.* (2005). Congenital endplate acetylcholinesterase deficiency responsive to ephedrine. *Neurology* **65**: 144–146.
11. Mihaylova, V, Müller, JS, Vilchez, JJ, Salih, MA, Kabiraj, MM, D'Amico, A *et al.* (2008). Clinical and molecular genetic findings in COLQ-mutant congenital myasthenic syndromes. *Brain* **131**(Pt 3): 747–759.
12. Feng, G, Krejci, E, Molgo, J, Cunningham, JM, Massoulié, J and Sanes, JR (1999). Genetic analysis of collagen Q: roles in acetylcholinesterase and butyrylcholinesterase assembly and in synaptic structure and function. *J Cell Biol* **144**: 1349–1360.
13. Lee, HH, Choi, RC, Ting, AK, Siow, NL, Jiang, JX, Massoulié, J *et al.* (2004). Transcriptional regulation of acetylcholinesterase-associated collagen ColQ: differential expression in fast and slow twitch muscle fibers is driven by distinct promoters. *J Biol Chem* **279**: 27098–27107.
14. Ruiz, CA and Rotundo, RL (2009). Dissociation of transcription, translation, and assembly of collagen-tailed acetylcholinesterase in skeletal muscle. *J Biol Chem* **284**: 21488–21495.
15. Inagaki, K, Fuess, S, Storm, TA, Gibson, GA, Mctiernan, CF, Kay, MA *et al.* (2006). Robust systemic transduction with AAV9 vectors in mice: efficient global cardiac gene transfer superior to that of AAV8. *Mol Ther* **14**: 45–53.
16. Nakai, H, Fuess, S, Storm, TA, Muramatsu, S, Nara, Y and Kay, MA (2005). Unrestricted hepatocyte transduction with adeno-associated virus serotype 8 vectors in mice. *J Virol* **79**: 214–224.
17. Bouma, SR, Drislane, FW and Huestis, WH (1977). Selective extraction of membrane-bound proteins by phospholipid vesicles. *J Biol Chem* **252**: 6759–6763.
18. Kimbell, LM, Ohno, K, Engel, AG and Rotundo, RL (2004). C-terminal and heparin-binding domains of collagenic tail subunit are both essential for anchoring acetylcholinesterase at the synapse. *J Biol Chem* **279**: 10997–11005.
19. Wang, Z, Zhu, T, Qiao, C, Zhou, L, Wang, B, Zhang, J *et al.* (2005). Adeno-associated virus serotype 8 efficiently delivers genes to muscle and heart. *Nat Biotechnol* **23**: 321–328.
20. Schnepp, BC, Clark, KR, Klemanski, DL, Pacak, CA and Johnson, PR (2003). Genetic fate of recombinant adeno-associated virus vector genomes in muscle. *J Virol* **77**: 3495–3504.
21. Kay, MA (2007). AAV vectors and tumorigenicity. *Nat Biotechnol* **25**: 1111–1113.
22. Xiao, X, Li, J and Samulski, RJ (1996). Efficient long-term gene transfer into muscle tissue of immunocompetent mice by adeno-associated virus vector. *J Virol* **70**: 8098–8108.
23. Rivière, C, Danos, O and Douar, AM (2006). Long-term expression and repeated administration of AAV type 1, 2 and 5 vectors in skeletal muscle of immunocompetent adult mice. *Gene Ther* **13**: 1300–1308.
24. Krejci, E, Legay, C, Thomine, S, Sketelj, J and Massoulié, J (1999). Differences in expression of acetylcholinesterase and collagen Q control the distribution and oligomerization of the collagen-tailed forms in fast and slow muscles. *J Neurosci* **19**: 10672–10679.
25. Lau, FT, Choi, RC, Xie, HQ, Leung, KW, Chen, VP, Zhu, JT *et al.* (2008). Myocyte enhancer factor 2 mediates acetylcholine-induced expression of acetylcholinesterase-associated collagen ColQ in cultured myotubes. *Mol Cell Neurosci* **39**: 429–438.
26. Arikawa-Hirasawa, E, Rossi, SG, Rotundo, RL and Yamada, Y (2002). Absence of acetylcholinesterase at the neuromuscular junctions of perlecan-null mice. *Nat Neurosci* **5**: 119–123.
27. Stum, M, Girard, E, Bangratz, M, Bernard, V, Herbin, M, Vignaud, A *et al.* (2008). Evidence of a dosage effect and a physiological endplate acetylcholinesterase deficiency in the first mouse models mimicking Schwartz-Jampel syndrome neuromyotonia. *Hum Mol Genet* **17**: 3166–3179.
28. Rotundo, RL, Rossi, SG and Anglister, L (1997). Transplantation of quail collagen-tailed acetylcholinesterase molecules onto the frog neuromuscular synapse. *J Cell Biol* **136**: 367–374.
29. Moretti, FA, Chauhan, AK, Iaconcig, A, Porro, F, Baralle, FE and Muro, AF (2007). A major fraction of fibronectin present in the extracellular matrix of tissues is plasma-derived. *J Biol Chem* **282**: 28057–28062.
30. Rooney, JE, Gurpur, PB and Burkin, DJ (2009). Laminin-111 protein therapy prevents muscle disease in the mdx mouse model for Duchenne muscular dystrophy. *Proc Natl Acad Sci USA* **106**: 7991–7996.
31. Hall, ZW and Ralston, E (1989). Nuclear domains in muscle cells. *Cell* **59**: 771–772.
32. Rossi, SG, Vazquez, AE and Rotundo, RL (2000). Local control of acetylcholinesterase gene expression in multinucleated skeletal muscle fibers: individual nuclei respond to signals from the overlying plasma membrane. *J Neurosci* **20**: 919–928.
33. Miner, JH, Go, G, Cunningham, J, Patton, BL and Jarad, G (2006). Transgenic isolation of skeletal muscle and kidney defects in laminin beta2 mutant mice: implications for Pierson syndrome. *Development* **133**: 967–975.
34. Somia, N and Verma, IM (2000). Gene therapy: trials and tribulations. *Nat Rev Genet* **1**: 91–99.
35. Mueller, C and Flotte, TR (2008). Clinical gene therapy using recombinant adeno-associated virus vectors. *Gene Ther* **15**: 858–863.
36. Helbling-Leclerc, A, Zhang, X, Topaloglu, H, Cruaud, C, Tesson, F, Weissenbach, J *et al.* (1995). Mutations in the laminin alpha 2-chain gene (LAMA2) cause merosin-deficient congenital muscular dystrophy. *Nat Genet* **11**: 216–218.
37. Nicole, S, Davoine, CS, Topaloglu, H, Cattolico, L, Barral, D, Beighton, P *et al.* (2000). Perlecan, the major proteoglycan of basement membranes, is altered in patients with Schwartz-Jampel syndrome (chondrodystrophic myotonia). *Nat Genet* **26**: 480–483.
38. Kawahara, G, Okada, M, Morone, N, Ibarra, CA, Nonaka, I, Noguchi, S *et al.* (2007). Reduced cell anchorage may cause sarcolemma-specific collagen VI deficiency in Ullrich disease. *Neurology* **69**: 1043–1049.
39. Okada, T, Nomoto, T, Yoshioka, T, Nonaka-Sarukawa, M, Ito, T, Ogura, T *et al.* (2005). Large-scale production of recombinant viruses by use of a large culture vessel with active gassing. *Hum Gene Ther* **16**: 1212–1218.
40. Okada, T, Shimazaki, K, Nomoto, T, Matsushita, T, Mizukami, H, Urabe, M *et al.* (2002). Adeno-associated viral vector-mediated gene therapy of ischemia-induced neuronal death. *Meth Enzymol* **346**: 378–393.
41. Okada, T, Nonaka-Sarukawa, M, Uchibori, R, Kinoshita, K, Hayashita-Kinoh, H, Nitahara-Kasahara, Y *et al.* (2009). Scalable purification of adeno-associated virus serotype 1 (AAV1) and AAV8 vectors, using dual ion-exchange adsorptive membranes. *Hum Gene Ther* **20**: 1013–1021.
42. Rohr, UP, Wulf, MA, Stahn, S, Steidl, U, Haas, R and Kronenwett, R (2002). Fast and reliable titration of recombinant adeno-associated virus type-2 using quantitative real-time PCR. *J Virol Methods* **106**: 81–88.
43. Engel, AG, Nagel, A, Walls, TJ, Harper, CM and Waisburg, HA (1993). Congenital myasthenic syndromes: I. Deficiency and short open-time of the acetylcholine receptor. *Muscle Nerve* **16**: 1284–1292.
44. Engel, AG and Santa, T (1971). Histometric analysis of the ultrastructure of the neuromuscular junction in myasthenia gravis and in the myasthenic syndrome. *Ann N Y Acad Sci* **183**: 46–63.
45. Engel, AG, Lindstrom, JM, Lambert, EH and Lennon, VA (1977). Ultrastructural localization of the acetylcholine receptor in myasthenia gravis and in its experimental autoimmune model. *Neurology* **27**: 307–315.
46. Otterness, IG and Chang, YH (1976). Comparative study of cyclophosphamide, 6-mercaptopurine, azathiopurine and methotrexate. Relative effects on the humoral and the cellular immune response in the mouse. *Clin Exp Immunol* **26**: 346–354.